JOURNAL OF ENVIRONMENTAL SCIENCES 40 (2016) 138–144

Available online at www.sciencedirect.com

ScienceDirect

www.elsevier.com/locate/jes

JES JOURNAL OF ENVIRONMENTAL SCIENCES

www.jesc.ac.cn

# Process analysis of characteristics of the boundary layer during a heavy haze pollution episode in an inland megacity, China

*Shan Wang*[1], *Tingting Liao*[2], *Lili Wang*[3], *Yang Sun*[3,*]

1. *Xi'an Meteorological Bureau, Xi'an 710016, China*
2. *Plateau Atmospheric and Environment Key Laboratory of Sichuan Province, College of Atmosphere Sciences, Chengdu University of Information Technology, Chengdu 610225, China*
3. *State Key Laboratory of Atmospheric Boundary Layer Physics and Atmospheric Chemistry (LAPC), Institute of Atmospheric Physics, Chinese Academy of Sciences, Beijing 100191, China*

ARTICLE INFO

*Article history:*
Received 30 July 2015
Revised 3 December 2015
Accepted 6 December 2015
Available online 11 January 2016

*Keywords:*
Haze
Temperature inversion
Radiation
Air stagnancy

ABSTRACT

Ground observation data from 8 meteorological stations in Xi'an, air mass concentration data from 13 environmental quality monitoring sites in Xi'an, as well as radiosonde observation and wind profile radar data, were used in this study. Thereby, the process, causes and boundary layer meteorological characteristics of a heavy haze episode occurring from 16 to 25 December 2013 in Xi'an were analyzed. Principal component analysis showed that this haze pollution was mainly caused by the high-intensity emission and formation of gaseous pollutants ($NO_2$, CO and $SO_2$) and atmospheric particles ($PM_{2.5}$ (fine particles) and $PM_{10}$ (respirable suspended particle). The second cause was the relative humidity and continuous low temperature. The third cause was the allocation of the surface pressure field. The presence of a near-surface temperature inversion at the boundary layer formed favorable stratification conditions for the formation and maintenance of heavy haze pollution. The persistent thick haze layer weakened the solar radiation. Meanwhile, a warming effect in the urban canopy layer and in the transition zone from the urban friction sublayer to the urban canopy was indicated. All these conditions facilitated the maintenance and reinforcement of temperature inversion. The stable atmospheric stratification finally acted on the wind field in the boundary layer, and further weakened the exchange capacity of vertical turbulence. The superposition of a wind field with the horizontal gentle wind induced the typical air stagnation and finally caused the deterioration of air quality during this haze event.



## Introduction

Along with the rapid socio-economic development, industrialization, urbanization, and traffic transport modernization in China recently, the demands for fossil fuels (*e.g.*, coals, petroleum and natural gas) have increased abruptly. Consequently, aerosol particles (direct emissions from vehicle exhaust, oil-burning, coal-burning, and waste combustion) react photochemically with gaseous pollutants to form secondary aerosol pollutants, which lead to a new type of disastrous weather in China, *i.e.*, haze and low-visibility events (Lin et al., 2014). According to statistics, China possesses four obvious haze-prone regions concentrated in the most developed regions, including the Beijing–Tianjin–Hebei region, Yangtze River

* *Corresponding author*. E-mail: suny@mail.iap.ac.cn (Yang Sun).

http://dx.doi.org/10.1016/j.jes.2015.12.008
1001-0742/

Delta, Pearl River Delta, and Sichuan Basin (Tao et al., 2013). This type of pollution is rapidly spreading from East China to midwest China, where central Shaanxi is becoming another haze-prone region.

Xi'an (107°40′ to 109°49'E, 33°29′ to 34°44'N, and 400 m above sea level) is located in Guanzhong Basin in the central Yellow River Basin in the inland area of mainland China. Xi'an, with total area of 9983 $km^2$ and an urban population of more than 8 million, is the capital city of Shaanxi Province and also the largest city in Northwest China. In this typical northern city, severe atmospheric pollution (Cao et al., 2005; Li and Feng, 2010; Shen et al., 2009) and frequently-occurring haze weather (Wang et al., 2014b) make Xi'an the most-polluted megacity in Northwest China. Pollution has severely harmed the urban environment and human health, and also strikingly impacted world-renowned cultural relics such as the Terra-Cotta Warriors (Cao et al., 2011).

A heavy haze weather process hit Xi'an consecutively from 16 to 25 December, 2013. The air quality index (AQI) exceeded 500 several times, reaching level six pollution, and Xi'an became the city with the worst air quality in China. In this study, we probed into the environmental quality characteristics, major influencing factors, and boundary layer meteorological characteristics of this heavy haze weather process.

## 1. Data and meteorological stations

The data used in this study included routine high-altitude data and ground data provided by MICAPS (meteorological information comprehensive analysis and process system); routine observations of radiosonde data and ground meteorological elements provided by Jinghe atmospheric observation station; and meteorological observation data from 7 observation stations (Xi'an, Zhouzhi, Huxian, Chang'an, Lantian, Lintong, and Gaoling) from 16 to 26 December, 2013. Other data included the wind profile radar data provided by the Chang'an atmospheric observation base in the south suburb of Xi'an; and the hourly monitored concentrations of $PM_{10}$ (respirable suspended particles), $PM_{2.5}$ (fine particles), $NO_2$, $SO_2$, CO, and $O_3$ provided from 13 air quality monitoring stations in Xi'an (Caotan, Qujiang, Guangyun Tan, Xingqing District, economic development zone, Chang'an District, Xi'an Stadium, Yanliang, Lintong, High-Voltage Switch Factory, textile zone, Xiaozhai, and Gaoxin). Specifically, the time intervals of ground observation and radiosonde were 1 and 12 hr respectively, at 08:00 and 20:00 (Beijing time); and the time interval of wind profile radar data was 6 min, at the measuring height of 6000 m. Fig. 1 shows the spatial distribution of all data observation stations.

## 2. Results and discussion

### 2.1. Characterization of air quality in heavy-polluted days

Based on the hourly monitored data from the 13 air quality monitoring sites in Xi'an, Fig. 2 shows the average hourly average concentrations of $PM_{2.5}$, $PM_{10}$, $SO_2$, $NO_2$, CO and $O_3$ in

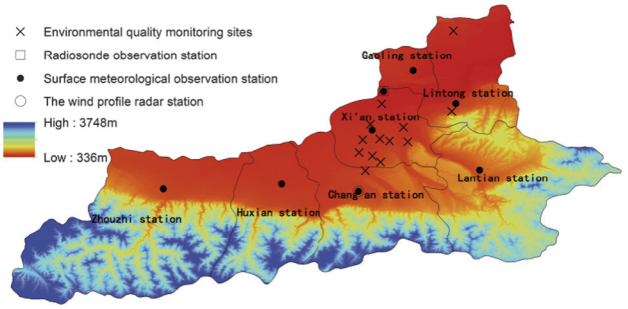


**Fig. 1 – Map of observation sites and geographical distribution in Shaanxi province.**

Xi'an, and the hourly curves of $PM_{2.5}/PM_{10}$ from 00:00 on day 16 to 10:00 on day 26, December 2013.

The mass concentrations of $PM_{2.5}$ and $PM_{10}$ changed basically in the same way, as both experienced a sustained growth stage, a high level stage, one limited clearance stage, and one rapid clearance stage. The consistent change trends indicate that the coarse and fine particles during the pollution period came from the same sources. Beginning at 00:00 on day 16, mass concentrations of $PM_{2.5}$ and $PM_{10}$ both increased in an undulating fashion and peaked at 478.2 and 692.9 $\mu g/m^3$ respectively at 21:00 on day 18. After the first cumulative growth, both $PM_{2.5}$ and $PM_{10}$ fluctuated around the peak levels. From 01:00 on day 20 to 23:00 on day 21, the concentrations of both $PM_{2.5}$ and $PM_{10}$ declined in an undulating pattern, but the clearance degrees were not very large. During this period, the lowest concentrations were 357.9 and 478.8 $\mu g/m^3$ respectively, indicating that the air quality in Xi'an was not much improved, but still severely deteriorated. Beginning on day 22, $PM_{2.5}$ and $PM_{10}$ gradually accumulated again, and the mass concentrations rapidly increased and peaked during this whole event at 21:00 on day 23 and at 13:00 on day 25 respectively (649.9 *vs.* 887.2 $\mu g/m^3$). These peak levels were 8.7 and 5.9 times higher respectively than the second-level standard thresholds in the Technical Regulation on Ambient Air Quality Index (on trial) (HJ633-2012) issued by the PRC (the People's Republic of China) Ministry of Environmental Protection, and were 26.0 and 17.7 times higher respectively than the 24-hr average thresholds provided by the World Health Organization (WHO). These comparisons indicate that the air quality in Xi'an deteriorated to an extremely low level. Beginning at 14:00 on day 25, the mass concentrations of $PM_{2.5}$ and $PM_{10}$ dropped rapidly, and decreased to 44.3 and 108.2 $\mu g/m^3$ respectively at 08:00 on day 26.

The ratio of $PM_{2.5}/PM_{10}$ reflects the enrichment degree of fine particles (Querol et al., 2004; Wang et al., 2007). During the first continuous accumulation of $PM_{2.5}$ and $PM_{10}$ particles, the ratio of $PM_{2.5}/PM_{10}$ experienced a complete peak-valley change process (Fig. 2). At 13:00 on day 16, the ratio of $PM_{2.5}/PM_{10}$ was maximized at 0.82, then sharply dropped, and was minimized at 0.44 at 10:00 on day 17. After that, the fine particles were obviously enriched again, and beginning at 00:00 on day 18, the $PM_{2.5}/PM_{10}$ ratio was stably maintained at a very high level (around 0.7). As reported, a higher $PM_{2.5}/PM_{10}$ ratio indicates more severe urban secondary pollution, and the ratio is 0.5–0.7 in heavily polluted cities (Maraziotis et al., 2008; Yang et al., 2011). Therefore, the $PM_{2.5}$ pollution in this study was mainly

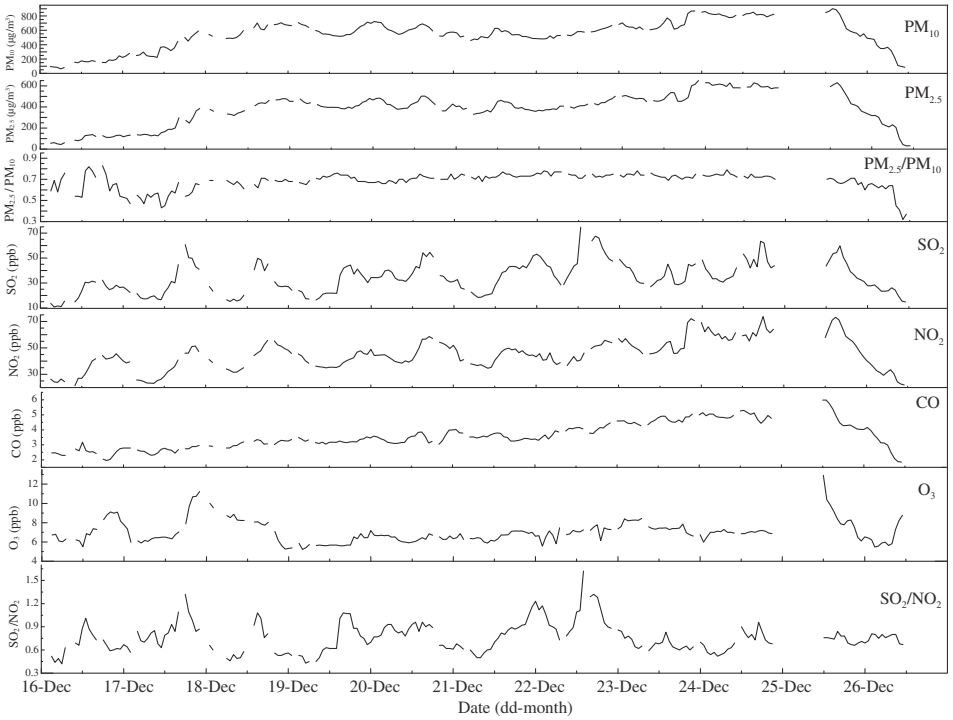


**Fig. 2 – Hour average concentration curves of $PM_{2.5}$ (fine particles), $PM_{10}$ (respirable suspended particles), $SO_2$, $NO_2$, CO, $PM_{2.5}/PM_{10}$ and $SO_2/NO_2$ from 16 to 26, December 2013 at Xi'an District.**

induced by fine particles, and displayed the general characteristics of typical $PM_{2.5}$ pollution in China.

### 2.2. Principal component analysis

The data on the air pollutants and meteorological factors associated with the polluting process of this heavy haze were evaluated by principal component analysis (PCA) in SPSS (Statistical Product and Service Solutions), and three major influence factors were found.

The first component included 5 air pollutants, *i.e.*, $NO_2$ (load 95.2%), $PM_{2.5}$ (90.1%), $PM_{10}$ (89.3%), CO (83.5%), and $SO_2$ (81.7%), indicating that these pollutants were highly associated but were not correlated with meteorological conditions. The correlation coefficients among the 5 pollutants (Table 1) show that under the joint impacts of regional transportation and local discharge, $SO_2$ and the other 4 pollutants were slightly correlated, while the other 4 pollutants were highly correlated, indicating similar sources. Besides the long distance transport, another major source of atmospheric $SO_2$ was the coal combustion during winter heating by residents. $NO_2$ and CO mainly reflect the exhaust emissions from vehicles, the coal consumption by residents, and the combustion of fossil fuels (*e.g.*, industrial oil) (Lee et al., 1997; Elansky, 2014; Xue et al., 2006). The sources of $PM_{2.5}$ and $PM_{10}$ are very complex and extensive. A quantitative source apportionment of $PM_{2.5}$ was carried out for winter 2013 in Xi'an and it was found that fossil emissions (from coal combustion and vehicle exhaust), biomass burning (including combustion of crop residues, heating and cooking), secondary emissions of other non-fossil sources, fugitive dust (originating from deserts in northwest China, construction sites and unpaved roads), and formation of secondary aerosol (from precursors such as $SO_2$, NO, and VOCs) mainly contributed to atmospheric particles (Zhang et al., 2015; Cao et al., 2012; Huang et al., 2014).

The second component included relative humidity (load 90.5%) and air temperature. The contribution of relative humidity to this event was only smaller than that of primary emissions, while the continuous low temperature was largely correlated with the aggravation of pollution. Along with the increase of relative humidity, the vapors would be more easily coagulated on aerosols and promote the hygroscopic growth of aerosols, which further intensified the heavy haze. At night, the vapors also inhomogeneously react with gaseous pollutants (*e.g.*, $NO_2$ and $SO_2$) to form inorganic particles (*e.g.*, nitrates and sulfates), which thereby adhere to haze particles and aggravate the pollution (Turšič et al., 2004; Gupta et al., 2008).

The third component includes air pressure (load 88.8%), which indicates that the weather background and the surface pressure field distribution induced by the circulation pattern play key roles in the formation and maintenance of this heavy

**Table 1 – Correlation index of atmospheric pollutants from 16 to 26, December 2013.**

| Correlation index | $PM_{2.5}$ | $PM_{10}$ | $SO_2$ | $NO_2$ | CO |
|---|---|---|---|---|---|
| $PM_{2.5}$ | 1.000 | 0.986** | 0.568* | 0.831** | 0.843** |
| $PM_{10}$ | | 1.000 | 0.559* | 0.826** | 0.820** |
| $SO_2$ | | | 1.000 | 0.725** | 0.496* |
| $NO_2$ | | | | 1.000 | 0.771** |
| CO | | | | | 1.000 |

$PM_{2.5}$: fine particles; $PM_{10}$: respirable suspended particle.
* 0.05 significance level test.
** 0.01 significance level test.

haze. During this pollution, the stagnant weather formed under a weak pressure field is unfavorable for the diffusion of pollutants, and the low pressure will facilitate the convergence of near-ground pollutants and aggravate pollution.

### 2.3. Temperature inversion at boundary layer

Fig. 3 shows the air temperature radiosonde curves at 08:00 and 20:00 from 16 to 25 December 2013 plotted on the basis of radiosonde observations from Jinghe station. Table 2 shows the thickness and intensity of the low-altitude temperature inversion layer at 08:00 and 20:00 in Xi'an on the basis of statistics. During this haze process, double or even multiple inversion occurred in most cases (Fig. 3). Specifically, under the influence of the southwest warm current, inversion layers appeared at medium to low altitude of 850–750 hPa; another temperature inversion layer appeared from ground to 950 hPa, especially ground inversion. At 08:00, the top of the near-ground inversion layer was usually located at 950 hPa: it had average thickness 226 m and inversion intensity at 0.5–1.6°C/100 m, and was generally thicker than that at 20:00 (Table 2). The lowest inversion layer at 20:00 was very thin and the height from the ground was smaller, and the average top height of inversion was 97 m, but the inversion intensity was larger (0.6–2.2°C/100 m). The existence of near-ground inversion stabilized the atmospheric stratification, and inhibited the vertical movement and turbulent exchange (Ye et al., 2015; Wang et al., 2014a). These changes would facilitate the near-ground accumulation of low-altitude vapors and aerosols, and provide sufficient condensation nuclei for the formation of haze (Wang et al., 2014a). Consequently, favorable stratification conditions were formed for the formation and maintenance of heavy haze pollution (Yang et al., 2015; Rao et al., 2008; Xie et al., 2010).

### 2.4. Radiation at boundary layer

The absorption and scattering of the haze would significantly reduce the surface solar radiation reaching the ground at daytime. From 16 to 25 December, the maximum total radiation was 4.568 MJ/m$^2$, but the value was 8.529 MJ/m$^2$ before or after this haze in other days of December, indicating that the daily radiation was attenuated by 46.4% and that the haze weather severely weakened the daytime solar radiation reaching the ground. In order to further confirm this phenomenon, we researched daily total radiation over 7 years, and found a value of 7.828 MJ/m$^2$ after eliminating the influence of clouds in the Xi'an region from 2006 to 2012 in the same period (16 to 25 December); by contrast, during the haze period of 16 to 25 December, 2013, the daily total radiation was attenuated by 41.6%. The great reduction of solar radiation severely weakened the warming effect of daytime solar radiation on the ground layers. From 16 to 25 December, the daily maximum temperature in Jinghe Station declined in an undulating fashion, and the average was only 3.1°C. Excluding days 26 to 28 with the occurrence of strong cold air, the average daily maximum temperature was only 30% of that in the non-haze days in December (10.3°C).

The radiosonde observations at 20:00 from Jinghe Station indicate that in December 2013 when the pollution of atmospheric particles reached level three and above, the urban canopy at 30 m height and the transition zone at 60 m height from the urban canopy to the urban friction sublayer were 0.82 and 1.07°C cooler respectively than the average ground temperature, which were all higher than the temperature differences in days with high air quality (0.68 *vs.* 0.96°C). A warming effect in the urban canopy layer and in the transition zone from the urban friction sublayer to the urban canopy is indicated here. As reported, absorptive aerosols can

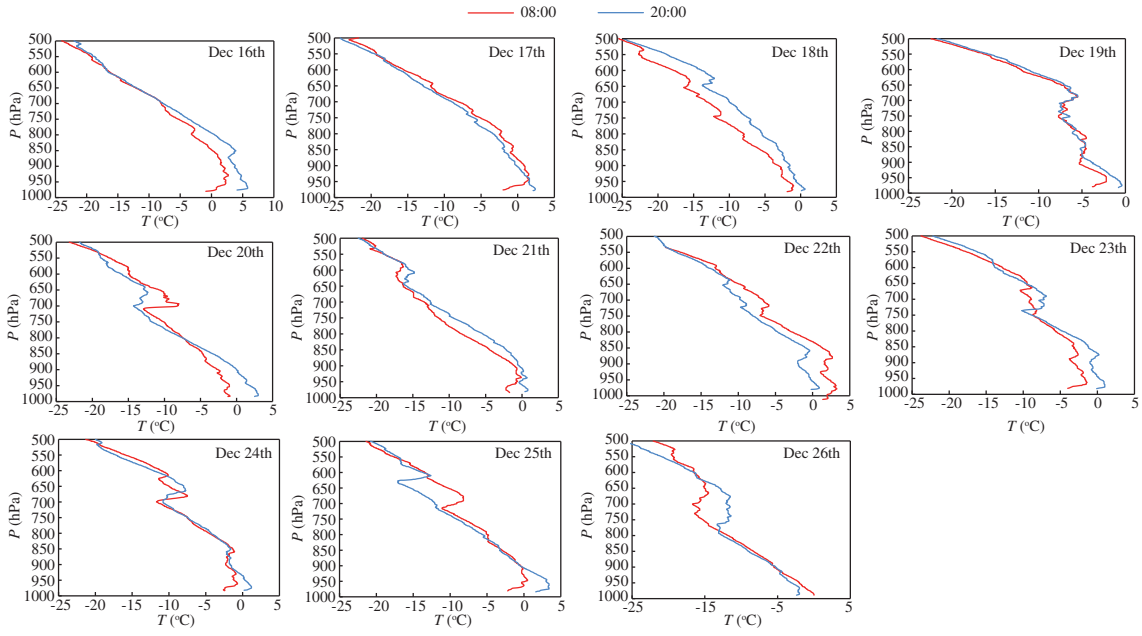


**Fig. 3 – Temperature (*T*) sounding curve of the Xi'an Jinghe river station on 08:00 and 20:00 every day from 16 to 25 December, 2013.**

**Table 2 – Thickness and strength of the temperature inversion in low altitude on 08:00 and 20:00 every day from 16 to 25, December 2013, Xi'an area.**

| Date | 08:00 | | 20:00 | |
|---|---|---|---|---|
| | Thickness (m) | Strength (°C/100 m) | Thickness (m) | Strength (°C/100 m) |
| 16 | 430* | 0.8 | 80* | 2.1 |
| 17 | 260* | 1.3 | – | – |
| 18 | 50* | 1.6 | 50* | 0.8 |
| 19 | 140* | 1.1 | 70* | 0.6 |
| 20 | 140 | 0.5 | 70* | 0.7 |
| 21 | 320 | 0.7 | 130* | 0.8 |
| 22 | 280* | 0.7 | 50* | 2.2 |
| 23 | 160* | 1.6 | 110* | 1 |
| 24 | 200* | 0.9 | 100* | 1 |
| 25 | 280* | 1 | 210* | 0.9 |

* Indicates grounding surface inversion.

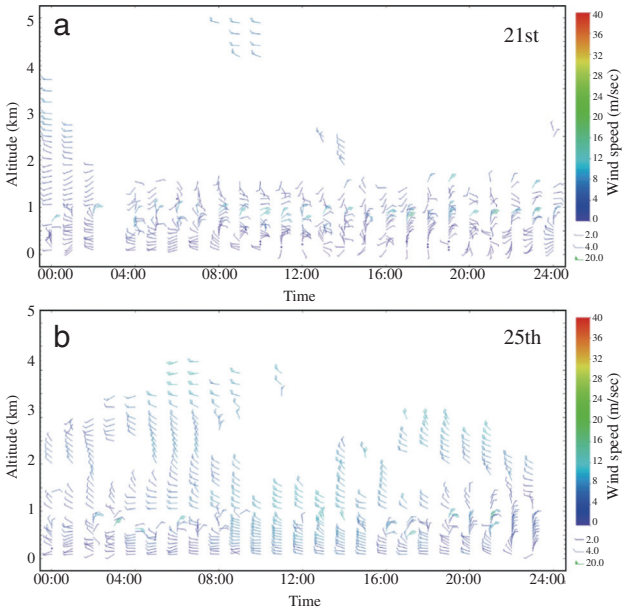


**Fig. 4 – Wind profile radar map at Changan atmospheric detection base on (a) day 21 and on (b) day 25, December 2013.**

directly absorb radiation and heat the layer of atmosphere where they are located (Hansen et al., 1997). During heavy haze pollution, the near-ground aerosols contain abundant black carbon substances formed from the incomplete combustion of fossils and biofuels, which originated from industry, transportation and winter heating by residents (Ramaswam et al., 2001; Hu et al., 2013). Black carbon, as the second or third single heating medium after only $CO_2$ and methane (Flanner et al., 2007; Latha and Badarinath, 2003), will strongly absorb solar radiation (Val Martín et al., 2006; Wu and Fu, 2005; Cartechini et al., 2015) and thus leads to positive radiative forcing, which was already validated (Ramaswam et al., 2001; Val Martín et al., 2006; Seki et al., 2015). The endothermic effect of absorptive aerosols including black carbon may be one of the reasons for the warming effect in the urban canopy layer and in the transition zone from the urban friction sublayer to the urban canopy, while this supposition should be confirmed through more observed data in future research.

The persistent low temperature reduced the daily range of air temperature, and weakened turbulent air exchange. Moreover, the warming effect in the urban canopy layer and in the transition zone from the urban friction sublayer to the urban canopy facilitated the maintenance and reinforcement of temperature inversion.

### 2.5. *Wind fields at boundary layer*

Stable air stratification will weaken the air diffusion ability in the vertical direction, which is reflected from the characteristics of the vertical wind field. Fig. 4 shows the typical wind profile radar maps during this haze weather process. Clearly, the low-altitude wind directions (<500 m) were very chaotic on 21 December (Fig. 4a), with weak wind speed and weak turbulence blending, which were typical wind fields, while they were favorable for the formation of haze. After 04:00 (UTC, Coordinated Universal Time), no echo data above 1500 m were observed, indicating very dry air and very weak turbulence; obvious wind shear occurred below 1000 m. The inconsistence of wind directions between upper and lower layers was unfavorable for the vertical/horizontal transport and diffusion of pollutants (Yang et al., 2015), which further aggravated the pollution. The direction of low-latitude wind above the station became a stable and consistent westerly wind starting on day 25, and the wind power was also enhanced. After 20:00 (UTC), the wind direction veered with height from the ground layer to 1000 m, but it backed with height from 1000 to 3000 m, indicating the presence of warm advection at low altitude, which was overlaid by cold advection. These conditions indicate that the atmospheric stratification started to destabilize. In the nighttime on day 26, along with the invasion of dry cold air, the stable air stratification was destroyed, and the near-ground turbulence and air diffusion abilities were enhanced, thus destroying the haze maintenance mechanism. The concentrations of atmospheric $PM_{2.5}$, $PM_{10}$, $SO_2$, $NO_2$, CO and $O_3$ greatly dropped and the AQI declined to second level (Good, according to the Technical Regulation on Ambient Air Quality Index (on trial) (HJ633-2012) issued by the PRC Ministry of Environmental Protection), indicating that the 10-day heavy haze pollution ended.

During the near-ground long-term low wind weather on day 21 with weak air turbulence and diffusion, this stagnant meteorological condition (Whiteman et al., 2014; Wang et al., 2008) will easily induce the formation of an airflow stagnant zone (Chen, 2012), which is unfavorable for the horizontal and vertical diffusion of pollutants. Consequently, the air pollutants accumulated rapidly, which provided abundant condensation nuclei for the formation of haze weather and promoted the long-term maintenance of heavy haze pollution (Wang et al., 2010). The frequently-occurring air stagnancy becomes one negative effect when climate changes slow down the atmospheric circulation (Horton et al., 2014). The 55-year wind speed changes in Xi'an (Fig. 5) indicate that the annual average wind speed is significantly decreasing at a rate of –0.2 m/sec/10 year

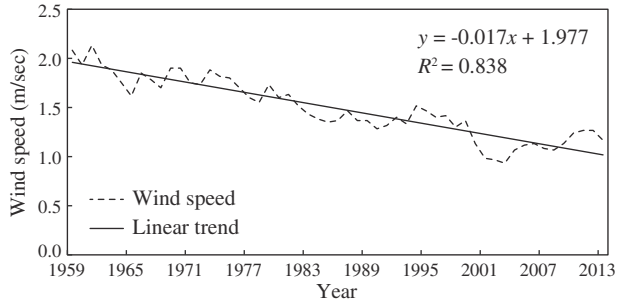


**Fig. 5 – Average wind speed curve in Xi'an area from 1959 to 2013.**

($R^2$ = 0.84). The slowdown of atmospheric circulation results in a weakened ground wind field, and more frequent occurrence of air stagnancy. The 46-year (1959–2004) data in Xi'an station show that the occurrence of calm wind increased in an undulating pattern at a rate of 4%/10 year ($R^2$ = 0.33) and was maximized to 72% in 2002. Thus, vertically stable atmospheric stratification combined with horizontal gentle winds induced the typical air stagnation (Horton et al., 2014) and caused the deterioration of air quality in this event.

## 3. Conclusions

Principal component analysis showed that this haze pollution was mainly caused by high-intensity emissions and formation of gaseous pollutants ($NO_2$, CO and $SO_2$) and atmospheric particles ($PM_{2.5}$ and $PM_{10}$). The second cause was the relative humidity and continuous low temperature. The third cause was the allocation of the surface pressure field.

The existence of near-ground inversion inhibited the vertical movement and turbulent exchange and thereby facilitated the near-ground accumulation of low-altitude vapors and aerosols. Consequently, favorable stratification conditions were formed, which promoted the formation and maintenance of heavy pollution. The persistent thick haze conversely weakened the daytime solar radiation reaching the ground, and weakened the near-ground heating effect. The persistent low temperature reduced the daily range of air temperature, and weakened the turbulent air exchange. Moreover, the warming effect in the urban canopy layer and the transition zone from the urban friction sublayer to the urban canopy facilitated the maintenance and reinforcement of temperature inversion. The 55-year wind speed changes in Xi'an (Fig. 5) indicate that the annual average wind speed is significantly decreasing at a rate of −0.2 m/sec/10 year. The occurrence of calm wind increased at a rate of 4%/10 year. These results indicate that the long-term climate changes in Xi'an have led to slower atmospheric circulation, weaker ground wind field, and higher frequency of air stagnancy. The stable atmospheric stratification finally acted on the wind field on the boundary layer, and further weakened the exchange capacity of vertical turbulence. The superposition of the wind field with the horizontal gentle wind induced the typical air stagnation and finally caused the deterioration of air quality during this haze event.

## Acknowledgments

This study was funded by the National Natural Science Foundation of China (Nos. 41175107, 41275139) and the "Strategic Priority Research Program" of the Chinese Academy of Sciences (Nos. XDA05100100, XDB05020000).

## REFERENCES

Cao, J.J., Wu, F., Chow, J.C., Lee, S.C., Li, Y., Chen, S.W., et al., 2005. Characterization and source apportionment of atmospheric organic and elemental carbon during fall and winter of 2003 in Xi'an, China. Atmos. Chem. Phys. 5, 3127–3137.

Cao, J.J., Li, H., Chow, J.C., Watson, J.G., Lee, S.C., Rong, B., et al., 2011. Chemical composition of indoor and outdoor atmospheric particles at Emperor Qin's Terra-cotta Museum, Xi'an, China. Aerosol Air Qual. Res. 11, 70–79.

Cao, J.J., Shen, Z.X., Chow, J.C., Watson, J.G., Lee, S.C., Tie, X.X., et al., 2012. Winter and Summer $PM_{2.5}$ chemical composition in fourteen Chinese cities. J. Air Waste Manage. Assoc. 62 (10), 1214–1226.

Cartechini, L., Castellini, S., Moroni, B., Palmieri, M., Scardazza, F., Sebastiani, B., et al., 2015. Acute episodes of black carbon and aerosol contamination in a museum environment: results of integrated real-time and off-line measurements. Atmos. Environ. 116, 130–137.

Chen, L.F., 2012. Climatic characteristics of haze in Hangzhou and intercomparison between haze process and cleaning process. Bull. Sci. Technol. 28 (7), 31–35.

Elansky, N., 2014. Air quality and CO emissions in the Moscow megacity. Urban Clim. 8, 42–56.

Flanner, M.G., Zender, C.S., Randerson, J.T., Rasch, P.J., 2007. Present-day climate forcing and response from black carbon in snow. J. Geophys. Res. 112 (D11), 10–1029.

Gupta, A.K., Karar, K., Ayoob, S., John, K., 2008. Spatio-temporal characteristics of gaseous and particulate pollutants in an urban region of Kolkata, India. Atmos. Res. 87 (2), 103–115.

Hansen, J., Sato, M., Ruedy, R., 1997. Radiative forcing and climate response. J. Geophys. Res. 102, 6831–6864.

Horton, D.E., Skinner, C.B., Singh, D., Diffenbaugh, N.S., 2014. Occurrence and persistence of future atmospheric stagnation events. 应为"*Nat. Clim. Change*." 4 (8), 698–703.

Hu, W., Hu, M., Tang, Q., Guo, S., Yan, C.Q., 2013. Characterization of particulate pollution during Asian Games in Pearl River Delta region. Acta Sci. Circumst. 33 (7), 1815–1823.

Huang, R.J., Zhang, Y., Bozzetti, C., et al., 2014. High secondary aerosol contribution to particulate pollution during haze events in China. 在"*Nature*"后面加. 514 (7521), 218–222.

Latha, K.M., Badarinath, K.V.S., 2003. Black carbon aerosols over tropical urban environment—a case study. Atmos. Environ. 69 (1), 125–133.

Lee, D.S., Köhler, I., Grobler, E., Rohrer, F., Sausen, R., Gallardo-Klenner, L., et al., 1997. Estimations of global NO, emissions and their uncertainties. Atmos. Environ. 31 (12), 1735–1749.

Li, X.P., Feng, L.N., 2010. Spatial distribution of hazardous elements in urban topsoils surrounding Xi'an industrial areas, (NW, China): controlling factors and contamination assessments. J. Hazard. Mater. 174, 662–669.

Lin, Y., Huang, K., Zhuang, G., Fu, J.S., Wang, Q., Liu, T., et al., 2014. A multi-year evolution of aerosol chemistry impacting visibility and haze formation over an Eastern Asia megacity, Shanghai. Atmos. Environ. 92, 76–86.

Maraziotis, E.S.L., Marazioti, C., Marazioti, P., 2008. Statistical analysis of inhalable (PM10) and fine particles (PM2.5)

concentrations in urban region of Patras, Greece. Glob. Nest J. 10 (2), 123–131.
Querol, X., Alastuey, A., Ruiz, C.R., Artiñano, B., Hansson, H.C., Harrison, R.M., et al., 2004. Speciation and origin of $PM_{10}$ and $PM_{2.5}$ in selected European cities. Atmos. Environ. 38 (38), 6547–6555.
Ramaswam, Y.V., Bou, C.O., Haigh, J., et al., 2001. Radiative forcing of climate change. Climate Change 2001: The Scientific Basis Contribution of Working Group I to the Third Assessment Report of the Intergovernmental Panel on Climate Change. Cambridge University Press, Cambridge, pp. 349–416.
Rao, X.Q., Li, F., Zhou, N.F., Yang, K.M., 2008. Analysis of a large-scale haze over Middle and Eastern China. Meteorol. Monogr. 34 (6), 89–96.
Seki, O., Kawamura, K., Bendle, J.A.P., lzawa, Y., Suzuki, L., Shiraiwa, T., et al., 2015. Carbonaceous Aerosol Tracers in Ice-cores Record Multi-decadal Climate Oscillations. Scientificreports/www.nature.com.
Shen, Z.X., Cao, J.J., Tong, Z., Liu, S.X., Reddy, L.S.S., Han, Y.M., et al., 2009. Chemical characteristics of submicron particles in winter in Xi'an. Aerosol Air Qual. Res. 9 (1), 80–93.
Tao, J., Zhang, L., Engling, G., Zhang, R., Yang, Y., Cao, J., et al., 2013. Chemical composition of $PM_{2.5}$ in an urban environment in Chengdu, China: importance of springtime dust storms and biomass burning. Atmos. Res. 122, 270–283.
Turšič, J., Berner, A., Podkrajšek, B., Grgić, I., 2004. Influence of ammonia on sulfate formation under haze conditions. Atmos. Environ. 38 (18), 2789–2795.
Val Martín, M., Honrath, R.E., Owen, R.C., Pfister, G., Fialho, P., Barata, F., 2006. Significant enhancements of nitrogen oxides, black carbon, and ozone in the North Atlantic lower free troposphere resulting from North American boreal wildfires. J. Geophys. Res. 111 (D23), 5525–5536.
Wang, Y., Zhuang, G., Chen, S., An, Z., Zheng, A., 2007. Characteristics and sources of formic, acetic and oxalic acids in $PM_{2.5}$ and $PM_{10}$ aerosols in Beijing, China. Atmos. Res. 84 (2), 169–181.
Wang, J., Fu, Q.Y., Wang, H.Z., Lu, T., Lin, C.Y., Feng, J., 2008. Study on an infrequent multi-day air pollution episode in Shanghai. Clim. Environ. Res. 13 (1), 53–60.
Wang, Y.F., Ma, Y.J., Lu, Z.Y., Li, C.J., Liu, N.W., 2010. Analysis of weather conditions and air pollution status during continuous fog days of Liaoning. Environ. Sci. Technol. 33 (6E), 289–291.
Wang, H., An, J., Shen, L., Zhu, B., Pan, C., Liu, Z., et al., 2014a. Mechanism for the formation and microphysical characteristics of submicron aerosol during heavy haze pollution episode in the Yangtze River Delta, China. Sci. Total Environ. 490c, 501–508.
Wang, S., Xiu, T.Y., Sun, Y., Meng, X.R., Xu, J.C., 2014b. The changes of mist and haze days and meteorological element during 1960–2012 in Xi'an. Acta Sci. Circumst. 34 (1), 19–26.
Whiteman, C.D., Hoch, S.W., Horel, J.D., Charland, A., 2014. Relationship between particulate air pollution and meteorological variables in Utah's Salt Lake valley. Atmos. Environ. 94, 742–753.
Wu, J., Fu, C.B., 2005. Simulation research of distribution transportation and radiative effects of black carbon aerosol in recent five spring, Chinese. J. Atmos. Sci. 29 (1), 111–119.
Xie, F.Y., Wang, Z.F., Wang, X.Q., 2010. A study of the characteristics of the synoptic situation and meteorological conditions in $PM_{10}$ air pollution episodes of Beijing during the 2008 Olympic Games period. Clim. Environ. Res. 15 (5), 584–594.
Xue, M., Wang, Y.S., Sun, Y., Hu, B., Wang, M.X., 2006. Measurement on the atmospheric CO concentration in Beijing. Environ. Sci. 27 (2), 200–206.
Yang, F., Tan, J., Zhao, Q., Du, Z., He, K., Ma, Y., et al., 2011. Characteristics of $PM_{2.5}$ speciation in representative megacities and across China. Atmos. Chem. Phys. 11 (11), 5207–5219.
Yang, Y., Liu, X., Qu, Y., Wang, J., An, J., Zhang, Y., et al., 2015. Formation mechanism of continuous extreme haze episodes in the megacity Beijing, China. Atmos. Res. 155, 192–203.
Ye, X., Wu, B., Zhang, H., 2015. The turbulent structure and transport in fog layers observed over the Tianjin area. Atmos. Res. 153, 217–234.
Zhang, Y.L., Huang, R.J., Haddad, I.E., Ho, K.F., Cao, J.J., Han, Y., et al., 2015. Fossil vs. non-fossil sources of fine carbonaceous aerosols in four Chinese cities during the extreme winter haze episode of 2013. Atmos. Chem. Phys. 15, 1299–1312.